ABSOLUTE VALUES OF INELASTIC NEUTRON SCATTERING CROSS-SECTIONS CALCULATED WITH ACCOUNT TAKEN OF THE PRE-EQUILIBRIUM MECHANISM

H. JAHN
Institut für Neutronenphysik und Reaktortechnik,
Kernforschungszentrum Karlsruhe G.m.b.H., and
Fakultät für Physik der Universität Karlsruhe,
Karlsruhe,
Federal Republic of Germany

Abstract

Absolute values of secondary energy-dependent inelastic neutron scattering cross sections can be calculated either with the master equation pre-equilibrium formalism of Cline and Blann or with Blann's more recent geometry-dependent hybrid model. The master equation formalism was used at Dubna and Dresden to reproduce experimental results for 14 MeV incident energy. The geometry-dependent hybrid model was used at Karlsruhe to cover for a number of materials the whole range from 5 to 14 MeV incident energy and to reproduce smoothed experimental spectra at 7.45 and 14 MeV. Only the geometry-dependent hybrid model accounts for scattering in the diffuse nuclear surface and thus for a certain average over the direct interaction. It is also free of any fit parameters other than those of the usual optical model. The master equation calculations, on the other hand, are based on nucleon-nucleon scattering cross sections inserted into the high-energy approximation of Kikuchi and Kawai for the intranuclear transition rate. Other approaches require either mass- or energy-dependent or more global fit parameters for a satisfactory reproduction of experimental results, but a genuine prediction of the incident-energy dependence of the inelastic neutron cross section, especially below 14 MeV, is needed for transport and shielding calculations for instance in connection with fusion reactor design studies.

1. Exciton master equation approach, achievements and shortcomings

1.1. Master equation

The first successful reproductions of energy distributions of nucleons emitted by excited nuclei were obtained by Griffin /1/ and Blann /2/ who applied phase space considerations to a sequence of steps of statistically treated particle-hole configurations. Cline and Blann /3/ extended this description to a more complete formalism by writing down a balance or master equation for the equilibrating compound nucleus. This master equation is still more or less the basis of various presently used models and codes for the calculation of spectra of inelastically scattered neutrons. We therefore briefly review this approach, starting with the master equation

$$(1) \qquad \frac{dP(n,t)}{dt} = P(n-2,t)\lambda_{+}^{n-2,n} + P(n+2,t)\lambda_{-}^{n+2,n} - P(n,t)(\lambda_{+}^{n,n+2} + \lambda_{-}^{n,n-2} + \lambda_{c}^{n,n-1}) \quad .$$

Here $P(n,t)$ is the probability per unit time that n excitons are excited at time t. The exciton number n is the sum of particles and holes,

$$(2) \qquad n = p + h \quad .$$

This excitation process developing step by step is illustrated by the following picture.

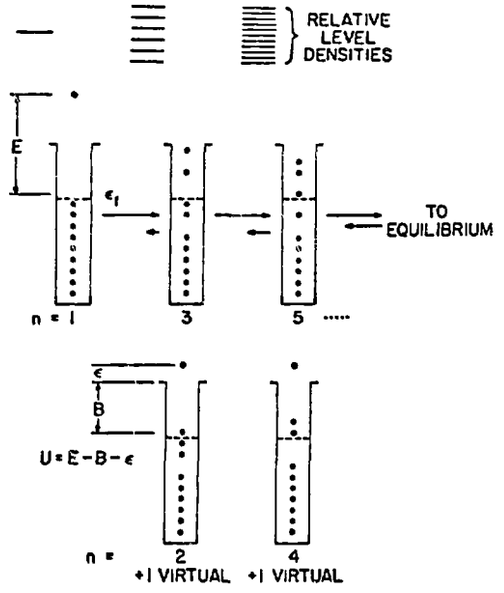

Fig. 1: Pictorial representation of the cascade equilibration process in the exciton model /4/.

Agassi, Weidenmüller and Mantzouranis /41/ showed how the master equation is related to the statistical theory of nuclear reactions. A different approach was developed by Bunakov (see Bunakov's lecture at this course).

The λ_+, λ_- in the master equation are the transition probabilities per unit time for an increase or decrease of the exciton number by one particle-hole pair while λ_c is the transition probability per unit time for the emission of a particle into the continuum from an n-exciton configuration.

If $w(n,\varepsilon)d\varepsilon$ is the probability for emission of a nucleon with an energy between ε and $\varepsilon+d\varepsilon$ from an n-exciton configuration then the total probability for emission of such a particle is given by

$$P(\varepsilon)d\varepsilon = \sum_n \int_0^\infty P(n,t)dt\, w(n,\varepsilon)d\varepsilon \,. \tag{3}$$

1.2. Closed-form approximation+)

Cline and Blann could show by full numerical calculation that the exact solution of the master equation can be approximated by

$$P(\varepsilon)d\varepsilon = \{C\, W(E,\varepsilon) + \sum_{n=n_0}^{\bar{n}} \tau_n\, w(n,\varepsilon)\}d\varepsilon \tag{4}$$

where τ_n is given by the expression

$$\tau_n = \frac{D_n}{\lambda_+^{n,n+2} + \lambda_-^{n,n-2}} \tag{5}$$

which shows that τ_n can be interpreted as the lifetime of an n-exciton state. D_n is the so-called depletion factor which still has to be determined, n_0 is the first-step exciton number - usually equal to 3 in the nucleon case - and $\bar{n}$ is the average exciton number when equilibrium is reached. Thus $\bar{n}$ is given by

$$\lambda_+^{\bar{n},\bar{n}+2} = \lambda_-^{\bar{n},\bar{n}-2} \,. \tag{5a}$$

The first term on the right-hand side of (4) is the equilibrium term with $W(E,\varepsilon)$ taken as the Weisskopf expression for the decay probability of an excited nucleus in equilibrium configuration /5/

$$W(E,\varepsilon)d\varepsilon = \sigma(E,\varepsilon)\frac{(2s+1)m\varepsilon}{\pi^2\hbar^3}\frac{\omega_B(U)}{\omega_A(E)}\,d\varepsilon \tag{6}$$

where s, m, ε are spin, mass and energy of the emitted particle.

The sum in (4) accounts for pre-equilibrium processes with $w(n,\varepsilon)$ chosen as the same Weisskopf expression, but now for the compound system in an n-exciton state instead of the equilibrium configuration. Thus (/2/, /4/, /5/)

$$w(n,\varepsilon)d\varepsilon = \sigma(E,\varepsilon)\frac{(2s+1)m\varepsilon}{\pi^2\hbar^3}\frac{\rho_{n-1}(U)}{\rho_n(E)}\,d\varepsilon \tag{7}$$

where $\rho_n(E)$ and $\rho_{n-1}(U)$ are the exciton state densities (number of states per energy interval) given by the Ericson expression /5a/

+) More detailed investigations about the master equation and its closed-form expression have been presented by Ribanský, Obložinský and Běták /42/.

$$\rho_n(E) = \frac{g(gE)^{-1}}{p!h!(n-1)!} \tag{7a}$$

for the excitation energy E of the compound nucleus and the excitation energy U of the residual nucleus, corresponding to the state densities $\omega_A(E)$ and $\omega_B(U)$ of the target nucleus A and the compound nucleus B in Eq. (6). The quantity g is the single-nucleon level density at the Fermi energy. In both equations (6) and (7) $\sigma(E,\varepsilon)$ is the absorption cross section of the nucleon to be emitted. With the binding energy B of the emitted particle we have

$$E = U + \varepsilon + B \tag{8}$$

as indicated in Fig. 1. The transition probability per unit time $\lambda_c^{n,n-1}$ for emission into the continuum from an n-exciton configuration is then given by

$$\lambda_c^{n,n-1} = \sum_i \left(\int_0^{E-B} w_i(n,\varepsilon)d\varepsilon \right)_i \tag{9}$$

where the sum extends over all types of emitted nucleons (i = n or p). The depletion factor D_n of Eq. (5) can now be expressed as

$$D_n = \prod_{n'=n_0+2}^{n} \left[1 - \sum_i \left(\int^{E-B} w(n'-2,\varepsilon)d\varepsilon \right)_i \right] . \tag{10}$$

The cross section for inelastic neutron scattering is obtained by multiplication of the total emission probability $P(\varepsilon)d\varepsilon$ of Eqs. (3) or (4) with the neutron absorption (compound nucleus formation) cross section $\sigma(\varepsilon_0)$ for the incident energy ε_0,

$$\sigma(\varepsilon_0,\varepsilon)d\varepsilon = \sigma(\varepsilon_0)P(\varepsilon)d\varepsilon \,. \tag{11}$$

1.3. Intranuclear transition rates with fit parameters

The transition probabilities λ_+ and λ_- in the master equation (1) remain to be determined. They are often discussed in a form which was first derived by Williams /6/ from the golden rule for transition probabilities,

$$\lambda_+^{n,n+2} = \frac{2\pi}{\hbar}|M|^2\frac{g^3E^2}{n+1}\,, \qquad \lambda_-^{n,n-2} = \frac{2\pi}{\hbar}|M|^2 g_{ph}(n-2) \,. \tag{12}$$

Here $|M|^2$ is the absolute square of the corresponding matrix element averaged over initial and final exciton states of excitation energy E. The factors behind $|M|^2$ are the phase space averages of the Ericson expression (7a) over final exciton states (phase space averages for a finite potential depth have been calculated by Běták and Dobeš /6a/). From the equilibrium condition (5a) and from (12) one gets for large n (for which p=h=n/2)

$$\bar{n} = \sqrt{2gE} \,. \tag{13}$$

$|M|^2$ is frequently treated simply as a fit parameter. In this case only relative spectral shapes rather than absolute cross sections can be calculated. A more elaborate prescription for the determination of $|M|^2$ is due to Braga-Marcazzan, Gadioli-Erba, Milazzo-Colli and Sona /7/ who used the Fermi gas model. As a result of this analysis and on the basis of her own studies Kalbach-Cline /8/ has proposed the following mass number and energy dependence

$$|M|^2 = KA^{-3}E^{-1} \tag{14}$$

which was also used by Strohmaier and Uhl /9/ for their own code STAPRE and by Young and Arthur /38/ for the code GNASH. The results of Kalbach-Cline for the constant K,

$$K = \begin{cases} 95\ \text{MeV}^3 \pm 32\% & \text{for nucleon-induced reactions,} \\ 725\ \text{MeV}^3 \pm 36\% & \text{for } \alpha\text{-particle-induced reactions} \end{cases} \tag{15}$$

show such large fluctuations that Uhl /9/ considered K as an adjustable parameter.

1.4. Intranuclear transition rates, effort to calculate absolute values

Blann /10/ and Braga-Marcazzan et al./7/ attempted to remove all adjustable parameters and thus to obtain absolute cross sections. They write

$$\lambda_+ = \rho v \langle\sigma\rangle \tag{16}$$

where ρ is the density of nucleons, v the particle velocity in nuclear matter and $\langle\sigma\rangle$ the effective cross section for an excited nucleon to interact with the other nucleons for which a Fermi gas momentum distribution is assumed. The average indicated by $\langle\ \rangle$ is taken over the free nucleon-nucleon scattering cross section with a method due to Goldberger /11/ and Hayakawa, Kawai and Kikuchi /12/ with the Pauli principle taken into account.

On this basis Gadioli, Gadioli-Erba and Sona /13/ calculated λ_+ for a truncated harmonic oscillator potential and for a square well, taking into account the finite potential depth not only for the exciton transition probabilities but also for the exciton state densities. For the harmonic oscillator well with 40 MeV Fermi energy at the center they found results which were only slightly different from those for the square well with 20 MeV Fermi energy. For the latter case their results are shown in Fig. 2.

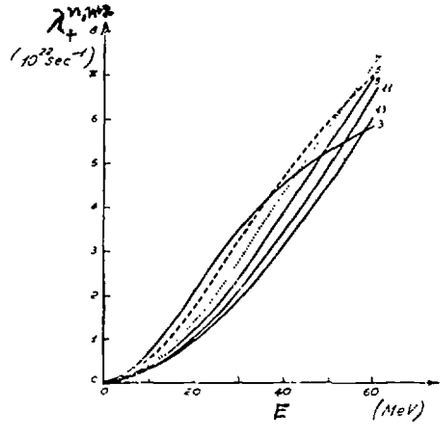

Fig. 2: Decay rates for the exciton-exciton interaction calculated in the framework of the Fermi gas model.

Fig. 2 shows a quadratic increase of $\lambda_+^{n,n+2}$ up to an excitation energy of 10 MeV and a linear increase above. This means that $|M|^2$ is independent of excitation below 10 MeV whereas above 10 MeV the energy dependence of Kalbach-Cline /8/ (see Eqs. (14), (15)) is confirmed.

In the case of the Fermi gas model and for a kinetic energy of relative motion higher than about 100 MeV $\langle\sigma\rangle$ can be represented by the following expression for a nucleon of type i (see /11/, /12/, /7/ and /13/),

$$\langle\sigma(E+E_F)\rangle_i = \left[(A-Z)\bar{\sigma}_{ni}(E+E_F) + Z\bar{\sigma}_{pi}(E+E_F)\right]/A \tag{17}$$

where

$$\bar{\sigma}_{ji}(E+E_F) = \sigma_{ji}(E+E_F)P(X); \qquad X = \frac{E_F}{E+E_F} \tag{18}$$

with

$$P(X) = \begin{cases} 1 - \frac{7}{5}X & \text{if } X \le \frac{1}{2} \\ 1 - \frac{7}{5}X + \frac{2}{5}X\,(2 - \frac{1}{X})^{5/2} & \text{if } X \ge \frac{1}{2} \end{cases} \tag{19}$$

and with the free nucleon-nucleon scattering cross section $\bar{\sigma}_{ji}$ which at the energy $E+E_F = mv^2/2$ can be represented as

$$\begin{aligned} \sigma_{nn}(E+E_F) &= \sigma_{pp}(E+E_F) = (10.63\ \beta^{-2} - 29.92\ \beta^{-1} + 42.9)\text{mb} \\ \sigma_{np}(E+E_F) &= \sigma_{pn}(E+E_F) = (34.10\ \beta^{-2} - 82.2\ \beta^{-1} + 82.2)\text{mb} \end{aligned} \tag{20}$$

where $\beta = v/c$ and c is the velocity of light (Metropolis et al. /14/, see also /12/).

With the Fermi energy E_F, the excitation energy E and the incoming-particle velocity in nuclear matter

$$v = \sqrt{\frac{2(E+E_F)}{m}} \tag{20a}$$

Gadioli, Gadioli-Erba and Sona /13/ were able to reproduce absolute values of secondary-energy-dependent (p,n) cross sections as well as excitation functions for a wide range of mass numbers ($89 \le A \le 169$) and excitation energies (15 MeV $\le E \le$ 50 MeV) provided they reduced their λ_+ values generally by a factor 4 ± 1.

Gudima, Osokov and Toneev /15/ did not need such a reduction factor. These authors replaced $E+E_F$ in σ_{ji} and v by the relative kinetic energy

$$T_n = \frac{8}{5}E_F + \frac{E}{n} \tag{21}$$

of the colliding particles in nuclear matter with n excitons and excitation energy E. Eq. (21) results from the so-called right-angle approximation. T_n is the sum of the mean kinetic energy of an excited particle (p)

$$T_n^{(p)} = E_F + \frac{E}{n} \tag{21a}$$

and the kinetic energy of an intranuclear nucleon (N) averaged over the Fermi spectrum,

(21b) $$T_n^{(N)} = \frac{3}{5} E_F .$$

Gudima, Osokov and Toneev /15/ achieved a good reproduction of the absolute values of the secondary-energy-dependent cross sections for the reactions Ta(n,n') at 14.6 MeV, Cu(α,p)Zn at 43 MeV and Ta(p,n)Zn at 18 MeV incident energy. Absolute pre-equilibrium (n,n') cross sections at 14 MeV were calculated in the same way by Hermsdorf, Meister, Sassonov, Seeliger and Seidel /16/ in good agreement with experimental results in the mass range $30 \leq A \leq 200$. The absorption cross section σ in Eqs. (6), (7) and (11) was obtained from the optical model. No additional fit parameters were needed but a λ_0 term was added to the master equation with

(12a) $$\lambda_0^{n,n} = \frac{2\pi}{\hbar} |M|^2 g^2 E \frac{3n-2}{2} .$$

Tests for more incident energies below as well as above 14 MeV and additional secondary-energy-dependent cross sections for a wide range of mass numbers should be performed before the predictive power of the method can be judged conclusively. This seems necessary in particular because the approximations (17)-(21a) were originally derived for kinetic energies of the colliding particles above about 100 MeV, which means for incident neutron energies above about 55 MeV if we consider $E+E_F$ as a measure for the relative energy of the colliding particles. The applications just mentioned, on the other hand, were made for incident neutron energies well below 55 MeV. Meanwhile Toneev has created a new "cascade exciton model" which is explained in Seeliger's lecture at this course. This model is able also to describe the angular distribution of the secondary particles.

2. Hybrid model approach

2.1. Pure hybrid model

An alternative to the approximations (16)-(21a) for λ_+ has been obtained by Blann /17/ who used the method of Kikuchi and Kawai /12/ to get a binomial function for nucleon energies up to about 100 MeV with the result

(22) $$\lambda_+(\varepsilon) = \{1.4 \cdot 10^{21} \text{ MeV}^{-1} (\varepsilon+B) - 6 \cdot 10^{18} \text{ MeV}^{-2} (\varepsilon+B)^2\} \text{ sec}^{-1}$$

This expression depends on the energy ε of the emitted nucleon. This means that Eqs. (4), (5) and (7) can no longer be interpreted as a closed-form approximation to the solution of the master equation. Instead Blann /17/ used Eq. (22) to obtain a marriage between the exciton model and the Harp-Miller-Berne model /18/ (see Bunakov's lecture at this course). This marriage, called by Blann the "hybrid model", produces the following simple expression for the total pre-equilibrium emission probability for a nucleon with an energy between ε and ε+dε:

(23) $$P_{pr}(\varepsilon)d\varepsilon = \sum_{\substack{n=n_0 \\ (\Delta n=2)}}^{\bar{n}} \frac{P_n}{p} \frac{\rho_{n-1}(U) g}{\rho_n(E)} \frac{\lambda_c(\varepsilon)}{\lambda_c(\varepsilon)+\lambda_+(\varepsilon)} D_n d\varepsilon .$$

In this expression one has

(24) $$\lambda_c(\varepsilon) = \frac{(2s+1)}{\pi^2\hbar^3} \frac{m\varepsilon\sigma(\varepsilon)}{g}$$

from which it can be seen that the numerator of (23) is almost the same as in Eq. (4) upon insertion of (5) and (7). One can also show that λ_c is the familiar transition probability into the continuum. The Weisskopf estimate is

(25) $$\lambda_c = W_A \frac{\omega_c}{g}$$

with the compound nucleus formation probability

(26) $$W_A = \frac{\sigma v}{V} = \frac{\sigma}{V} \sqrt{\frac{2\varepsilon}{m}}$$

where V is the laboratory volume, $v = \sqrt{2\varepsilon/m}$ the particle velocity and σ the inverse absorption cross section. With the state density of the continuum corresponding to the laboratory volume V, viz.

(27) $$\omega_c = (2s+1) \frac{Vm^{3/2}}{\pi^2\hbar^3} \sqrt{\frac{\varepsilon}{2}}$$

and the single-nucleon level density g as given by (7a) one obtains in fact Eq. (24). Eq. (23) can be interpreted in the following way: The first factor in the sum is the fraction of nucleons of a given type (neutrons or protons) that is to be emitted. The second factor counts the number of allowed arrangements leading to emission into the secondary-energy interval between ε and ε+dε after scattering of the considered nucleon in the nuclear matter of the excited nucleus (with n excitons). Blann could show that the result of this counting for $n>5$ can be approximated by the result given by Ericson /5a/ or Williams /20/ for the n-exciton state density

(7b) $$\rho_n(E) = \frac{g(gE-\theta)^{n-1}}{p!h!(n-1)!}$$

with the constant single-particle level density g referring to an infinitely deep potential well, usually taken at the Fermi energy,

(7c) $$g = \frac{3A}{2E_F} .$$

The quantity θ is a correction term for the Pauli principle which could be neglected in all cases that have been investigated, and D_n in (23) is given by

(28) $$D_n = \prod_{n_0+2<n'<n}^{n} \left\{1 - \sum_i \left\{ \int_0^{E-B} P_{n'}(\varepsilon)d\varepsilon \right\}_i \right\}$$

where $P_{n'}(\varepsilon)d\varepsilon$ is the n-th *sum* term in (23) and the *summation* extends over nucleon types.

A successful reproduction of experimental emission cross sections for (α,p) reactions, integrated over angles but dependent on secondary energy, was obtained by Mignerey and Blann /4/ and by Chevarier et al. /21/ according to Eqs. (11), (23), (22), and (24) without any parameter adjustment except for n_0 (see Fig. 3).

2.2. Influence of nuclear surface diffuseness, ALICE and OVERLAID ALICE

Results for the angle-integrated secondary-energy-dependent cross section for the reaction ^{197}Au(p,p') are shown in Fig. 4 (from Ref. /22/). The calculated values obtained with the choice $n_0 = 3$ disagree very much with the measured

data. The choice $n_0 < 3$, however, appears quite unphysical unless we assume that at the nuclear surface one of the three excitons (a hole) is suppressed. Such an assumption can be understood in the framework of the Thomas-Fermi model,

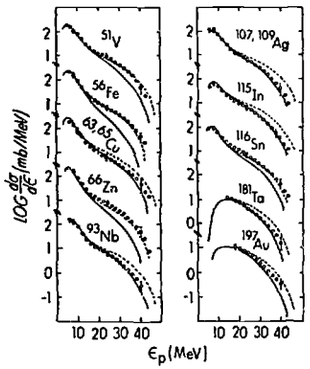

Fig. 3: Experimental and calculated (α,p) cross sections for 55 MeV incident α-particle energy (from Ref. /21/). The points represent experimental angle-integrated cross sections given as a function of secondary proton energy. The dashed lines are hybrid-model results with $n_0 = 4$, the solid lines with $n_0 = 5$. Equilibrium components are included in the calculated spectra.

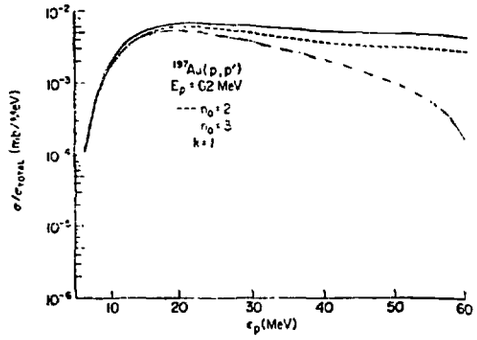

Fig. 4: Experimental and calculated $^{197}Au(p,p')$ cross sections for 62 MeV incident protons. Experimental results (Ref. /23/) are given by the solid curve, calculated results by the dashed line for $n_0 = 2$ and by the dotted line for $n_0 = 3$.

if the Fermi energy, as in the atomic case, is taken as decreasing with the nuclear density d(r) towards the surface according to

$$E_F(r) = \frac{\hbar^2}{2m}\left(\frac{3}{2}\pi^2 d(r)\right)^{2/3} \tag{29}$$

where the density follows the Fermi (or Woods-Saxon) distribution

$$d(r) = d_s\left\{e^{(r-c)/z} + 1\right\}^{-1} \tag{30}$$

with the nuclear half-density radius

$$c = c_0 A^{1/3}, \qquad c_0 = 1.07 \text{ fm}, \tag{30a}$$

the surface thickness

$$z = 0.55 \text{ fm} \tag{30b}$$

and the saturation density

$$d_s = \left(\frac{4\pi}{3} c_0^3\right)^{-1}. \tag{30c}$$

A reasonable way to account for the influence of the nuclear surface diffuseness can be obtained according to Blann /24/ by averaging along the particle trajectory taking the impact parameter

$$R_\ell = \ell\lambda \tag{31}$$

as the lower limit and the upper limit as

$$R_s = c + 5z \tag{32}$$

outside the nucleus where the density is practically zero. The quantities ℓ and λ in (31) are the orbital angular momentum quantum number and the de Broglie wave length,

$$\lambda = \frac{\hbar}{\sqrt{2m\varepsilon_0}}. \tag{33}$$

The averaged density is then defined by

$$d(R_\ell) = \frac{1}{R_s - R_\ell}\int_{R_\ell}^{R_s} d(r)dr. \tag{34}$$

Inserting this into the Fermi energy expression (29) one gets the geometry-dependent Fermi energy or potential depth

$$E_F(R_\ell) = E_F\cdot\left(\frac{d(R_\ell)}{d_s}\right)^{2/3} \tag{35}$$

where

$$E_F = \frac{\hbar^2}{2m}\left(\frac{3\pi^2}{2} d_s\right)^{2/3} \tag{36}$$

is the usual Fermi energy.

From the good results obtained without surface diffuseness for (α,p) reactions by Mignerey and Blann /4/ and Chevarier et al. /21/ with $n_0 = 4$ or 5 (see Fig. 3) and from the failure with $n_0 = 3$ in the case of $^{197}Au(p,p')$ (see Fig. 4) Blann /25/ concluded that only for $n_0 = 3$ (incident nucleons) must the surface diffuseness be taken into account because only then can an exciton acquire enough energy to sense the bottom of the potential well. In this way Blann /25/ found

$$(37)\qquad \rho_{1p1h} = gE_F(R_\ell), \qquad U > E_F(R_\ell);$$
$$\rho_{2p1h} = \frac{1}{4} g^2 E_F(R_\ell)\{2E-E_F(R_\ell)\}, \quad E > E_F(R_\ell).$$

The Ericson (7a) or Williams formula (7b) is used in all other cases.

In addition there is an influence of the surface diffuseness on the third factor in each sum term of Eq. (23): g in the expression (24) for $\lambda_c(\varepsilon)$ has to be taken as

$$(38)\qquad g(R_\ell) = \left(\frac{\varepsilon+B+E_F(R_\ell)}{E_F}\right)^{1/2} \frac{2N}{A} g$$

instead of (7c). Finally also the absorption and excitation rate $\lambda_+(\varepsilon)$ in the third factor of Eq. (23) can be affected by the surface diffuseness. This is the case if $\lambda_+(\varepsilon)$ is calculated from the imaginary part W(r) of the optical potential for neutron scattering according to

$$(39)\qquad \lambda_+^{(\ell)}(\varepsilon) = \frac{2W(R_\ell)}{\hbar} \quad \text{with} \quad W(R_\ell) = \frac{1}{R_s-R_\ell}\int_{R_\ell}^{R_s} W(r)dr \ .^{+)}$$

One can now calculate the pre-equilibrium component of the inelastic-scattering neutron cross section, integrated over emission angles but dependent on the secondary energy, by means of the Eqs. (23), (7b), (7c), (28), (31)-(39). These equations represent the hybrid model with surface diffuseness which was called by Blann the geometry-dependent hybrid model. Apart from general nuclear parameters such as nucleon numbers (N, Z, A), nuclear radius and surface thickness the model contains only the optical-model quantities W and $\sigma(\varepsilon)$. In particular there are no additional fit parameters. Moreover, the geometry-dependent hybrid model is the only existing model that takes the diffuseness of the nuclear surface into account.

A computer code was developed by Blann /26/ on the basis of this model the first version of which was called ALICE /26/. In this code, as in Refs. /24/ and /25/, the expression

$$(40)\qquad g(R_\ell) = \frac{3A}{2E_F(R_\ell)}$$

was used instead of (38). This led to unrealistic results as described in Ref. /29/. The calculations of Hansen, Grimes, Howerton and Anderson (see Ref. /37/) were apparently based on Eq. (40) and therefore give too small pre-equilibrium components of the secondary-energy-dependent inelastic neutron-scattering cross section. Also our own first (n,n') calculations on ^{56}Fe and ^{238}U with the hybrid model code /26/ were only successful after re-introduction of a fit parameter /39/.

+) In (39) R_s is given by $R_s = r_o A^{1/3}+5a$ with $r_o = 1.32$fm and $a = 0.51+0.7(N-Z)/A$ which is somewhat different from (32).

This deficiency of ALICE was corrected in the version OVERLAID ALICE /27/ which was successfully applied to (p,p') reactions by Blann (see Ref. /4/) and to d-, ^{3}He- and ^{4}He-induced reactions by Bisplinghoff, Ernst, Machner, Mayer-Kuckuk and Jahn, Probst, Djaloeis, Davidson and Mayer-Böricke (see Ref. /4/).

Further applications to angle-integrated secondary energy distributions for the reactions $^{55}Mn(n,n')$, $^{56}Fe(n,n')$, $^{58}Ni(n,n')$ and $^{93}Nb(n,n')$ will be presented below (see Refs. /28/, /29/ and /30/).

2.3. Equilibrium component

Before comparison with experimental data is possible one has to add an equilibrium component to the pre-equilibrium expression (23). In ALICE and OVERLAID ALICE the Weisskopf evaporation formula is used. In our own calculations we used instead the more accurate angle-integrated Hauser-Feshbach expression for continuous channels,

$$(41a)\qquad \left(\frac{d\sigma(\varepsilon_0,\varepsilon)}{d\varepsilon}\right)_{eq} = \pi\lambda^2 \frac{\sum_\ell (2\ell+1)T_\ell(\varepsilon_0)\sum_{\ell'} T_{\ell'}(\varepsilon)\omega(\varepsilon_0-\varepsilon)/2}{\sum_{\ell'}\{\sum_{U_{\nu'}} T_{\ell'}(\varepsilon_0-U_{\nu'}) + \int_0^{\varepsilon_0-\varepsilon_c} T_{\ell'}(\varepsilon)\omega(\varepsilon_0-\varepsilon)d\varepsilon/2\}}$$

The neutron transmission coefficients T_ℓ were calculated with the Perey-Buck /31/ optical-model program and also used for the calculation of $\sigma(\varepsilon)$ in Eqs. (11), (23) and (24). The density of residual excited states $\omega(\varepsilon_0-\varepsilon)$, with the excitation energy of the residual nucleus given by

$$(41b)\qquad \varepsilon_0-\varepsilon = \begin{cases} U & \text{for the continuum,} \\ U_{\nu'} & \text{for discrete levels,} \end{cases}$$

and ε_c being the continuum cut-off, was taken as

$$(41c)\qquad \omega(U) = \begin{cases} e^{(U-U_0)/T} & \text{for } U \le U_x \ , \\ \dfrac{e^{2\sqrt{a(U-\Delta)}}}{12\sqrt{2}c\sqrt{(U-\Delta)^3}} a^{3/2} & \text{for } U \ge U_x \ , \end{cases}$$

with

$$(41d)\qquad c/a = 0.0888\, A^{2/3}$$

and

$$(41e)\qquad a/A = (0.00917\, S + \begin{cases} 0.142 \\ 0.120 \end{cases}) \text{ MeV}^{-1} \text{ for } \begin{cases} \text{spherical nuclei} \ , \\ \text{deformed} \quad " \quad . \end{cases}$$

The other constants in (41c)-(41e) are taken from tables presented by Gilbert and Cameron /32/ from whose work these level-density expressions were adopted in the MELENE program /33/.

2.4. Numerical results for inelastic neutron scattering

The final result ist obtained by adding equilibrium and pre-equilibrium components,

$$(42)\qquad \frac{d\sigma(\varepsilon_0,\varepsilon)}{d\varepsilon} = \left(\frac{d\sigma(\varepsilon_0,\varepsilon)}{d\varepsilon}\right)_{eq} + \left(\frac{d\sigma(\varepsilon_0,\varepsilon)}{d\varepsilon}\right)_{pr} .$$

The numerical results are presented in Figs. 5a-e for the target nuclei ^{52}Cr, ^{55}Mn, ^{56}Fe, ^{58}Ni and ^{93}Nb. The sum curves as well as the equilibrium and pre-equilibrium curves are plotted together with the experimental histograms. The incident energy in all these cases was $\varepsilon_0 = 14.6$ MeV. The histograms were obtained from experimental results by averaging over 1 MeV energy intervals of the scattered neutrons. In the case of ^{56}Fe the measurements were performed at Livermore /34/. The histograms for the other nuclei were obtained by angular integration of data measured at Dresden /35/ for angles of 40^o, 60^o, 90^o, 120^o and 150^o in the case of Cr and Nb, and for 52.9^o, 77.7^o, 89.9^o, 108.4^o and 131.1^o in the case of Mn and Ni. We carried out the angle integration after interpolating between the cross section data given at those angles with the help of

$$\frac{d^2\sigma(\varepsilon_0,\varepsilon,\theta)}{d\varepsilon d\Omega} = \sum_{\ell=0}^{5} a_\ell P_\ell(\cos\theta) \quad (43)$$

The coefficients a_ℓ of the Legendre polynomials $P_\ell(\cos\theta)$ were determined by fitting the measured cross section values.

2.5. Discussion

The results given in Figs. 5a-5e show that the measured data are reproduced quite well by our calculations as far as the pre-equilibrium component is concerned. This is also true for the equilibrium component in the case of Fe, Cr and Mn, where the sum curve fits the experimental values over the whole range of secondary energies. For ^{58}Ni, however, the contribution of the (n,p) channels cannot be neglected in the Hauser-Feshbach denominator (eq. (41a)) as we have done. The Q-value for the (n,p) reaction is exceptionally low in this case. Therefore the calculated equilibrium part is too large compared with the measured data. On the other hand the relatively low negative Q-value of the (n,2n) processes for ^{93}Nb shows that these cannot be neglected as we did. The calculated equilibrium part in this case is too small. The completion of our calculations in this respect is underway.

2.6. Incident energy dependence

The data considered so far were obtained with 14.6 MeV neutrons. Below this incident energy there is a gap without data down to 8.56 MeV. Below the gap there are measurements again, performed at Oak Ridge between 4.19 and 8.56 MeV /36/. The gap must be filled by model calculations. Blann's geometry-dependent hybrid model appears to be a proper tool for this purpose because it yields absolute cross sections from the optical model alone without any undetermined parameters. A check against the data below the gap confirms the usefulness of the model: Fig. 6 shows calculated and measured cross sections for the reaction $^{56}Fe(n,n')$ as a function of residual excitation energy, for an incident energy of 7.54 MeV. Our model-calculated results are drawn as a smooth line through the fluctuating curve measured at Oak Ridge /36/. It can be seen that the calculated curve is close to an average of the measured values. This is at the same time a strong indication that the geometry-dependent hybrid model with Hauser-Feshbach term describes the dependence on incident energy of the angle-integrated, secondary-energy-dependent inelastic neutron cross section adequately. The model can therefore be used to close the gap, at least in the sense of averages over intermediate structure. For $^{56}Fe(n,n')$ this interpolation has been used to calculate the inelastic scattering cross section data which have been incorporated in the KEDAK library (see ref. /46/).

2.7. Direct component

Since especially the high-energy tails of the angle-integrated secondary spectra are quite well reproduced by our results it looks as if the direct scattering contribution is already included in Blann's geometry-dependent hybrid model.

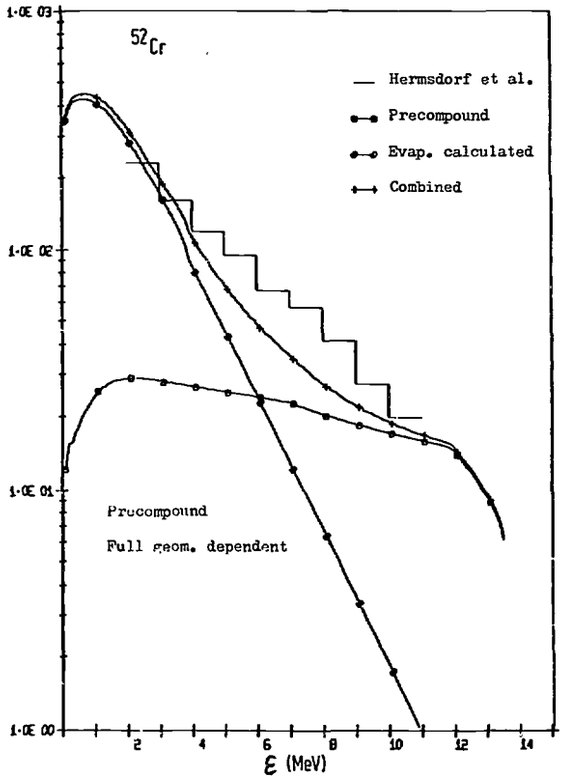

Fig. 5a: Angle integrated energy distribution of inelastic 14.6 MeV neutron cross section of ^{52}Cr.

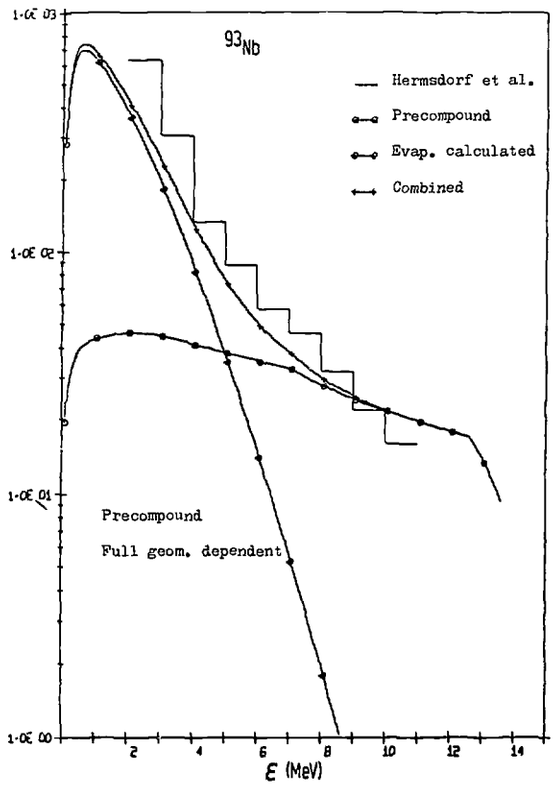

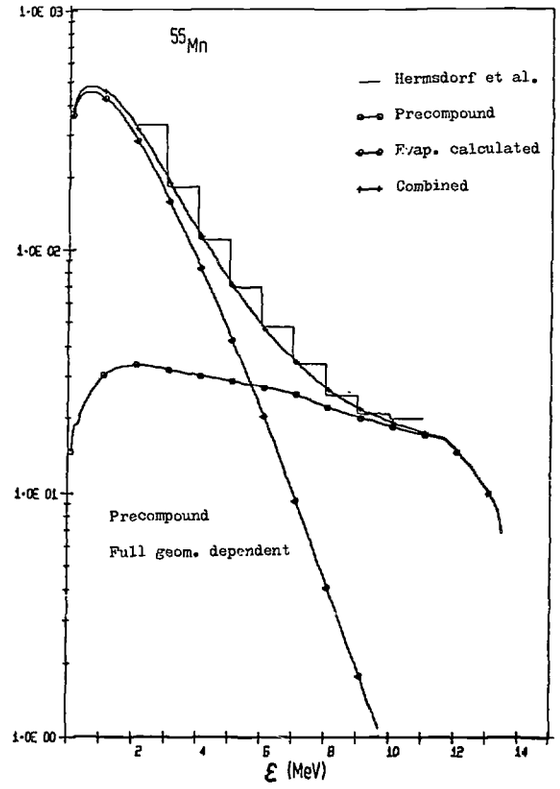

Fig.5b and c: Angle integrated energy distribution of inelastic 14.6 MeV neutron cross section of ^{93}Nb and ^{55}Mn.

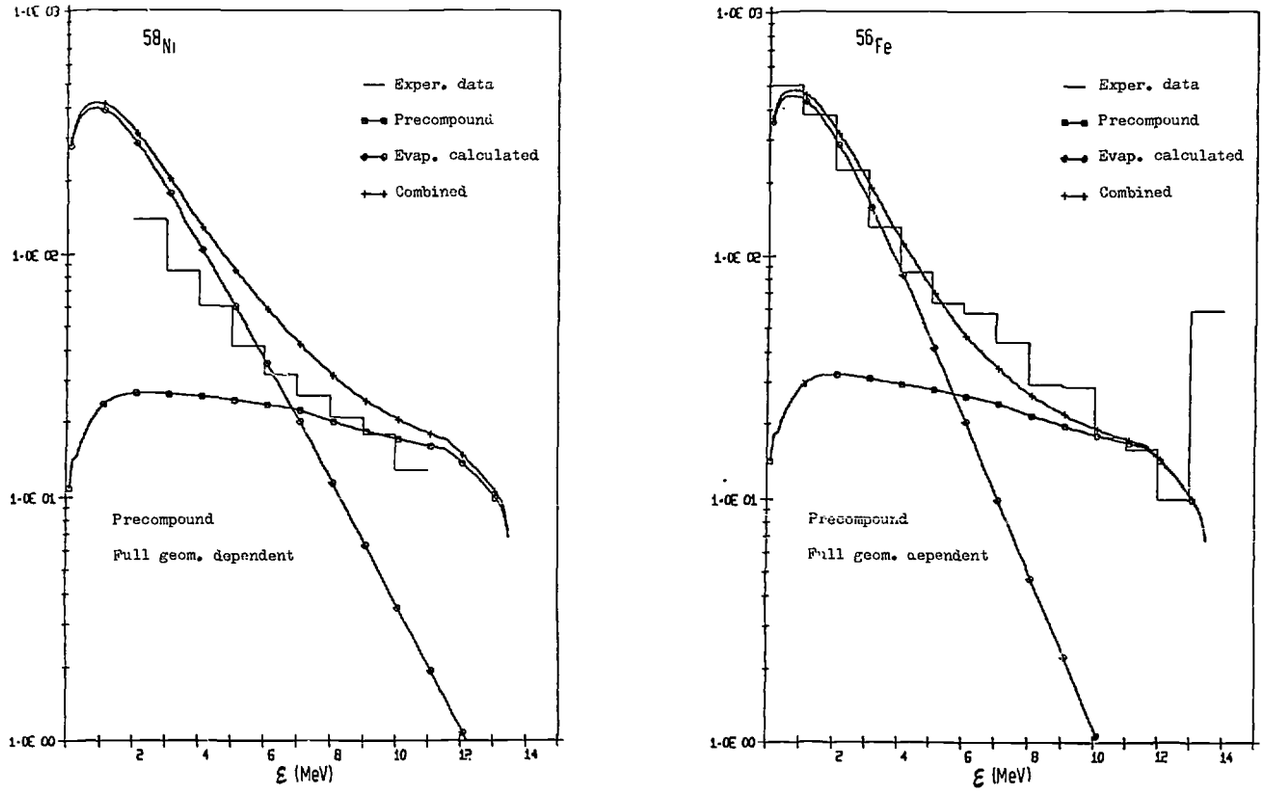

Fig.5d and e: Angle integrated energy distribution of inelastic 14.6 MeV neutron cross section of ^{58}Ni and ^{56}Fe.

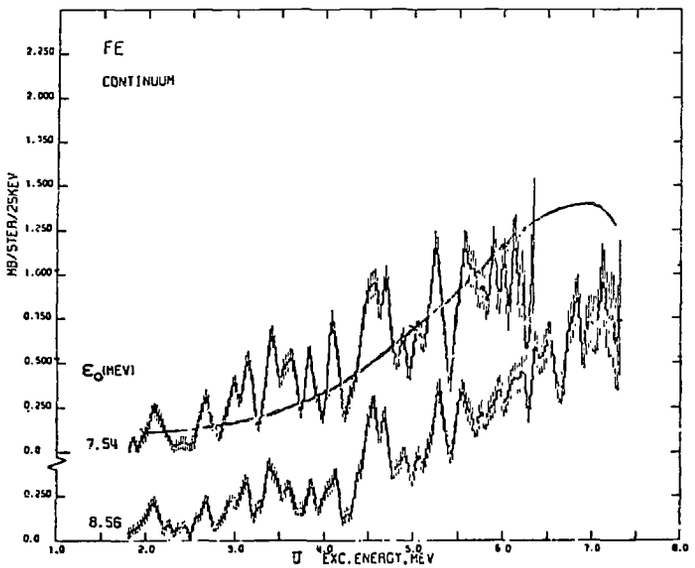

Fig.6: The angle-averaged continuum differential inelastic-scattering cross sections per 25 keV per atom of natural iron for the two contaminant-free sets of measurements of the Oak Ridge group /36/. The solid line represents the results of our calculations.

This point was discussed in a previous paper /29/. Actually, for the case of nucleon-induced reactions, Blann interprets the lowest-order ($n_0 = 3$) contribution from three-exciton pre-equilibrium states as a direct component in the geometry-dependent version of his hybrid model. We have tested this interpretation by checking whether the angular distribution of the high-energy tail (energy averaged over 1MeV intervals as before) can be described on this basis. For this purpose we have written down the energy- and angle-dependent differential cross section as composed of three components,

$$(44) \qquad \frac{d^2\sigma(\varepsilon_0,\varepsilon,\theta)}{d\varepsilon d\Omega} = \frac{1}{4\pi}\left(\frac{d\sigma(\varepsilon_0,\varepsilon)}{d\varepsilon}\right)_{eq} + \frac{1}{4\pi}\left(\frac{d\sigma(\varepsilon_0,\varepsilon)}{d\varepsilon}\right)_{n\geq 5} + \left(\frac{d^2\sigma(\varepsilon_0,\varepsilon,\theta)}{d\varepsilon d\Omega}\right)_{dir} .$$

The equilibrium component is considered as isotropic as well as the pre-equilibrium component from states with more than three excitons. The third component, however, is considered as the direct component, and consequently we choose for it the angular dependence given by the plane wave Born approximation,

$$(45) \qquad \left(\frac{d^2\sigma(\varepsilon_0,\varepsilon,\theta)}{d\varepsilon d\Omega}\right)_{dir} = F(\varepsilon_0,\varepsilon)\sqrt{\frac{\varepsilon}{\varepsilon_0}}(2\ell'+1)\sum_L C_{\ell\ell'}(L0,00)j_L^2(QR)$$

where $Q = |\vec{k}_0 - \vec{k}|$ is the absolute value of the momentum transferred to the target nucleus (in units of $\hbar$), the $j_L(QR)$ are spherical Bessel functions and the $C_{\ell\ell'}$ are Clebsch-Gordan coefficients. The factor $F(\varepsilon_0,\varepsilon)$ is determined by equating the angle-integrated direct part with the 3-exciton contribution of the geometry-dependent hybrid model according to

$$(46) \qquad \int d\Omega \left(\frac{d^2\sigma(\varepsilon_0,\varepsilon,\theta)}{d\varepsilon d\Omega}\right)_{dir} = \left(\frac{d\sigma(\varepsilon_0,\varepsilon)}{d\varepsilon}\right)_{n=3} .$$

The results are shown together with the measured angular distributions of the Dresden group /35/ in Fig. 7. Since many 2^+ states of ^{56}Fe are excited in the considered energy intervals we have put $L = 2$ for this rough test. In view of the approximations made the agreement is quite satisfactory. The lowest-order term in Blann's exciton expansion appears in fact to be responsible for the direct-reaction contribution. It is emphasized once more that our results with the geometry-dependent hybrid model were obtained, without any fit parameters, exclusively from conventional optical-model information. This remarkable success encourages further refinement of the model. The occurence of direct processes as indicated by Eqs. (44)-(46) and Fig. 7 can also be seen from recent work by Feshbach /40/. Also the similarity of the averaged spectral shape of DWBA - with geometry-dependent hybrid results at 90° scattering angle and 17 MeV incident energy which was found for the ^{116}Sn(p,p')-process by Arndt and Reif /43/ supports his concept.

In contrast to the above outlined concept the direct component has been treated by Lukyanov, Salnikov and Saprykin /44/, by Fu /45/ and in ref. /28/ as unrelated to the pre-equilibrium component. While the pre-equilibrium compoent is completely omitted in the evaporation + DWBA-fit of Lukyanov et al. /44/ it has been shown very clearly by Fu /45/ that the experimental Livermore spectrum of Fig. 5e cannot be reproduced by absolute Hauser-Feshbach + DWBA-calculations alone unless a pre-equilibrium component is added. Fu has done it by fitting Blann's first exciton estimate /2/. As the other way around the pre-equilibrium component has been calculated absolutely using the pure hybrid model in ref. /28/ and the experimental energy spectral shape of Fig. 5e could very well be reproduced using in addition a PWBA-fit of the Dresden experimental angular distribution.

Acknowledgement

The author wants to express his best gratitude to his collegue Dr. F. Fröhner for much help by reading and preparing the manuscript. Informative discussions with Dr. D. Rusch are also gratefully acknowledged.

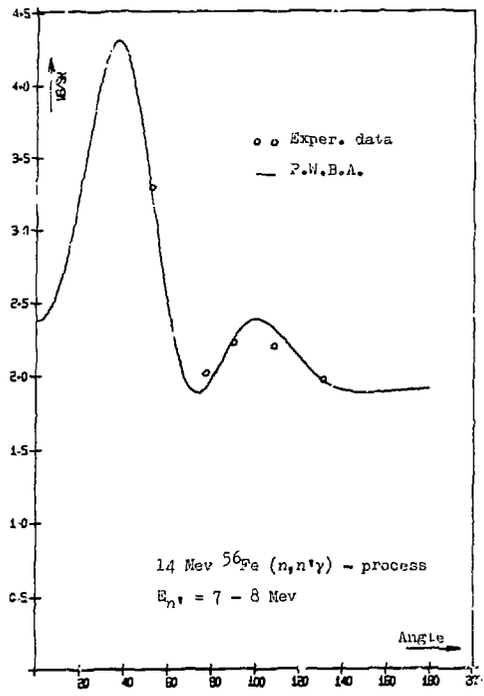

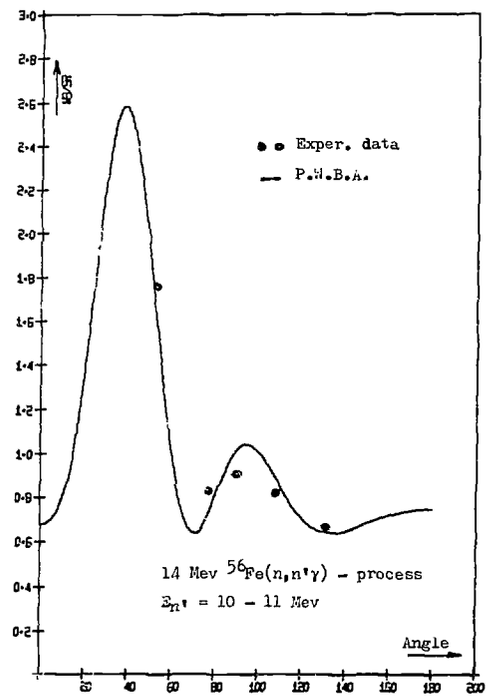

Fig.7: Angular distribution of 14 MeV neutrons scattered inelastically on ^{56}Fe. The curves represent a PWBA distribution with equilibrium + $n \geq 5$ pre-equilibrium background where the angle-integrated PWBA component is equated with the n_o=3 component of the geometry-dependent Hybrid model.

References

/1/ Griffin,J.J., Phys. Rev. Lett. 17,478 (1966); Int. Nucl. Phys. Conf., 1966, Gatlinburg Tenn. ed. R.L. Becker p.778, New York Academic; Intermediate Structure in Nuclear Reactions, ed. H.P. Kennedy, R. Schrils, Lexington: Univ. Kentucky Press, 219 pp. Phy. Lett.B, 24, 5 (1967)

/2/ Blann, M., Phys. Rev. Lett. 21, 1357 (1968); Blann, M., Lanzafame, F.M. Nucl. Phys. A 142.559 (1970)

/3/ Cline, C.K., Blann, M., Nucl. Phys. A 172, 225 (1971); Cline,C.K., Nucl.Phys.A.193, 417 (1972), Nucl. Phys. A.195, 353 (1972).

/4/ Blann, M., Ann. Rev. Nucl. Sci. 25, 123 (1975)

/5/ Weisskopf, V.F., Phys. Rev. 53, 295 (1937) Weisskopf V.F. and Ewing D. Phys. Rev. 57, 472 and 935 (1940)

/5a/Ericson, T., Adv. Phys. 9,423 (1960)

/6/ Williams, Phys. Lett. B31, 184 (1970)

/6a/Běták, E., Dobeš, J.,Z. Phys. A. 279, 319 (1976)

/7/ Braga-Marcazan, G.M., Gadioli-Erba, E., Milazzo-Colli, L. and P.G. Sona, Phys. Rev. C6, 1398 (1972)

/8/ Kalbach-Cline, C., Nucl. Phys. A 210, 570, 1973

/9/ Strohmaier, B. and Uhl,M. see lectures of this courses and Uhl, M. in Nuclear Theory in Neutron Nuclear Data Evaluation, IAEA-190, Vol.II, p.361

/10/Blann, M., Phys. Rev. Lett., 27, 337 (1971), 700E, 1550 E

/11/Goldberger, M., Phys. Rev. 74, 1269 (1948)

/12/Kikuchi, K., Kawai, M. Nuclear Matter and Nuclear Interactions, North-Holland Publishing Comp., Amsterdam 1968, S.33-40

/13/Gadioli, E., Gadioli-Erba, E., and Sona, P.G., Nucl. Phys. A 217,589 (1973), see Proc. Int. Conf. on Nucl. Reaction Mechanism, Varenna, June 13-17,1977, p.24

/14/Metropolis, N., Bivins, R., Storm, M., Miller, J.M., Friedländer, G. and Turkevich, A., Phys. Rev.110, 204, 185 (1958); 166,949 (1968).

/15/Gudima, K.K., Osokov, G.A., Toneev, V.D., Sov.J.Nucl.Phys. 21, 138 (1975)

/16/Hermsdorf, D., Meister, A., Sassonov, S., Seeliger, D., Seidel, K. in Nuclear Theorie in Neutron Nuclear Data Evaluation 1975/76, IAEO-190, p.274,283; ATOMKI, Közlemények 18, 229 (1976)

/17/Blann, M. see ref. /10/ and Blann, M. and Mignerey, A., Nucl. Phy. A. 186, 245 (1972)

/18/Harp, G.D., Miller, J.M. Phys. Rev. C3, 1847 (1971)

/19/Blann, M., Mignerey, A. and Scobel W. Proc. 8th International Summer School in Nuclear Physics, Mikocaki, Poland (1975); Nukleonika 21, 335 (1976)

/20/Williams, F.C. Jr., Nucl. Phys. A 166, 231 (1971)

/21/ Chevarier, A., Chevarier, N., Demeyer, A., Hollinger, G. and Tran Minh Duc, Phys. Rev.C.8, 2155 (1973)

/22/ Blann, M., Mignerey, A. Nucl. Phys. A 186, 245 (1972)

/23/ Bertrand , F.E. and Peelle, R.W., see ref. /22/

/24/ Blann, M., Nucl. Phys. A 213,570 (1973)

/25/ Blann, M., Phys. Rev. Lett. 28, 757;see also the comments in Phys.Rev.C17,1871u.2238 (1978)

/26/ Blann, M., Hybrid Code, US-AEC Report No. COO-3494-9 (1973), see also ref. /24/, Blann, M. and Plasil, F., ALICE a Nuclear Evaporation Code, US-AEC Report No. COO-3494-10 (1973)

/27/ Blann, M., OVERLAID ALICE, USERDA Report No. COO-3494-29 (1976); Additions and Corrections to OVERLAID ALICE, USERDA Report No. COO-3494-32 (1976)

/28/ Jahn,H.,Broeders,C.H.M.,Broeders,I. , Proc. Conf. Nuclear Cross Sections and Technology, Washington D.C., March 3-7, 1975, p.350, N.B.S. Sp. Pub.425

/29/ Jahn,H., in Nuclear Theory in Neutron Nuclear Data Evaluation, Trieste, 1975/76, IAEA-190, Voll.II p.315

/30/ Jahn, H., C.H.M. Broeders and I. Broeders in Proc. Int. Conf. on Nucl. Reaction Mechanism, Varenna, June 13-17, 1977, p. 185

/31/ Perey, F., ORNL 3429, (1963)

/32/ Gilbert, A., Cameron, A.G.W., Can Journ. Phys. 43, 144 (1965)

/33/ Penny, S.K., HELENE, ORNL-TM-2590 (1969)

/34/ Hansen, L.F., Anderson, I.D., Brown, P.S., Howerton, R.I., Kemerdiener, I.L., Logan, C.M., Plechaty, E.F. and Wong, C., Nucl. Sc. Eng. 51, 278 (1973)

/35/ Hermsdorf, D., Meister, A., Sassonov, S., Seeliger, D., Seidel, V. and Shahin, F., Kernenergie 17, 259 (1974), ZfK-277

/36/ Kinney, W.E., and Perey, F.G., ORNL-4515 (1970)

/37/ Hansen, L.F., Grimes, S.M., Howerton, R.J. and Anderson, J.D., Nucl. Sc. Eng. 1,201 (1961)

/38/ Young, P.G. and Arthur, E.D., LA-6947, UC-34c, Nov.1977

/39/ C.H.M. Broeders,I.Broeders,H.Jahn and M.Lalovic AERE-R 8636,NEANDC(UK) 170L NEACRP L176(1977),Proc.Spec.Meeting on Inelastic Scattering and Fission Neutron spectra held at AERE, Harwell April 14-16 1975

/40/ Feshbach,H.,in Proc. Int. Conf.on Nucl. Reaction Mechanism, Varenna, June 13-17, 1977,

/41/ Agassi,D.,Weidenmüller,H.A.,Mantzouranis,G.,Physics Reports 22C,147 (1975)

/42/ Ribanský,I., Obložinský,P. and Běták,E., Nucl. Phys. A205,545 (1973); A226, 347 (1974)

/43/ Arndt,E. and Reif,R., see ref. /29/ p.353

/44/ Lukyanov,A.A., Salnikov, O.A. and Saprykin,E.M., Sov.J.Nucl.Phys.21, 35 (1975)

/45/ Fu,C.F., see ref. /28/ p. 328

/46/ Fröhner,F.H., Broeders,C., Broeders,I., Goel,B., Langer,I., Meyer,R., Wiese,H.W., KfK 2387/V.